PHENOLIC PLANT EXTRACT ENRICHMENT OF ENZYMATICALLY MINERALIZED HYDROGELS

Timothy E.L. Douglas[1,2,3]*, Marco A. Lopez-Heredia[4], Aleksandra Pułczyńska[5], Agata Łapa[5], Krzysztof Pietryga[5], David Schaubroeck[6], Sónia A.O. Santos[7], Adriana Pais[7], Gilles Brackman[8], Karel De Schamphelaere[9], Sangram Keshari Samal[10,11], Julia K. Keppler[12], Jonas L. Bauer[12], Feng Chai[4], Nicolas Blanchemain[4], Tom Coenye[8], Elżbieta Pamuła[5], Andre G. Skirtach[1,11]

[1] Dept. Molecular Biotechology, Ghent University, Belgium
[2] Engineering Department, Lancaster University, United Kingdom
[3] Material Science Institute (MSI), Lancaster University, United Kingdom
[4] U1008: Controlled Drug Delivery Systems and Biomaterials, Univ. Lille II, France
[5] Dept. Biomaterials and Composites, AGH University of Science and Technology, Kraków, Poland
[6] Centre for Microsystems Technology (CMST), imec and Ghent University, Belgium
[7] CICECO-Aveiro Institute of Materials, Dept. Chemistry, University of Aveiro, Portugal
[8] Laboratory of Pharmaceutical Microbiology, Ghent University, Belgium
[9] Laboratory for Environmental and Acquatic Ecology, Ghent University, Belgium
[10] Laboratory of General Biochemistry and Physical Pharmacy, Ghent University, Belgium
[11] Centre for Nano- and Biophotonics, Ghent University, Belgium,
[12] Dept. Food Technology, Christian-Albrechts-Universität zu Kiel, Germany
*e-mail: t.douglas@lancaster.ac.uk

Abstract

Hydrogel mineralization with calcium phosphate (CaP) and antibacterial activity are desirable for applications in bone regeneration. Mineralization with CaP can be induced using the enzyme alkaline phosphatase (ALP), responsible for CaP formation in bone tissue. Incorporation of polyphenols, plant-derived bactericidal molecules, was hypothesized to provide antibacterial activity and enhance ALP-induced mineralization. Three phenolic rich plant extracts from: (i) green tea, rich in epigallocatechin gallate (EGCG) (herafter referred to as EGCG-rich extract); (ii) pine bark and (iii) rosemary were added to gellan gum (GG) hydrogels and subsequently mineralized using ALP. The phenolic composition of the three extracts used were analyzed by ultra-high-performance liquid chromatography coupled to tandem mass spectrometry (UHPLC-MS^n). EGCG-rich extract showed the highest content of phenolic compounds and promoted the highest CaP formation as corroborated by dry mass percentage meassurements and ICP-OES determination of mass of elemental Ca and P. All three extracts alone exhibited antibacterial activity in the following order EGCG-rich > PI > RO, respectively. However, extract-loaded and mineralized GG hydrogels did not exhibit appreciable antibacterial activity by diffusion test. In conclusion, only the EGCG-rich extract promotes ALP-mediated mineralization.

Keywords: *hydrogel, mineralization, polyphenols, antibacterial, epigallocatechin gallate, gellan gum*

[Engineering of Biomaterials 149 (2019) 2-9]

Introduction

Hydrogels are 3D polymer structures, or networks, in which a high amount of liquid is introduced [1]. These materials present the advantage of being loaded with active molecules, drugs and/or cells. In addition, the properties of hydrogels can be tailored by modifying the polymer network composing the hydrogel or their cross-linking mechanism [2,3]. Gellan Gum (GG) is made of polysaccharide anionic polymer which can be used as the networks for obtaining hydrogels [4,5]. Mineralization of this type of hydrogels with calcium phosphate (CaP) is desirable for applications in bone regeneration. One mineralization strategy is incorporation of the enzyme alkaline phosphatase (ALP) to cleave phosphate from glycerophosphate (GP) substrate upon incubation in a solution containing Ca^{2+} and GP, resulting in CaP formation in the hydrogel [6].

In addition to this mineralization capacity, antibacterial properties are desirable for bone regeneration materials as the increasing prevalence of antibiotic-resistant bacteria, *e.g.* methicillin-resistant *Staphylococcus aureus* Mu50 (MRSA), is a major concern in clinic [7,8]. Flavonoids, *i.e.* a sub-class of polyphenols occurring in fruit, vegetables, nuts, seeds, stems, flowers and tea, exhibit antibacterial activity in addition to other properties such as antioxidant, anti-inflammatory, anti-mutagenic and anti-carcinogenic properties [9,10]. The mechanism of action of several flavonoids has been investigated [9], being known that their structure and concentration can affect the ALP and cell activities [11]. Previously, incorporation of a macroalgae phenolic extract into GG hydrogels promoted subsequent ALP-induced mineralization and endowed antibacterial activity before and after mineralization [6]. Quercetin and apigenin have been object of particular interest amongst flavonoids due to their antibacterial properties [10].

In this work, two well-known plant extracts, namely green tea extract, rich in epigallocatechin gallate (EGCG), hereafter referred to EGCG-rich extract, and rosemary extract (RO), and a less studied extract, i.e. pine bark (PI, Pycnogenol) were added to GG hydrogels. GG hydrogels were subsequently mineralized using ALP. We hypothesized that these extracts would promote CaP formation and endow antibacterial activity. In fact, green tea extract has shown antibacterial activity against both Gram-positive and Gram-negative bacteria [12]. Pine bark and rosemary extracts have been also reported to show antibacterial activity, ascribed by the authors to the presence of polyphenols [13], and phenolic acids [14], respectively. Notwithstanding, green tea, rosemary and pine bark extracts were characterized by ultra-high-performance liquid chromatography with diode array detector and coupled to an ion trap mass spectrometer (UHPLC-DAD-MS^n). Promotion of mineralization was assessed by measurement of dry mass percentage, *i.e.* mass percentage of mineralized hydrogels attributable to mineral and polymer and not water, by Inductively Coupled Plasma Optical Emission Spectroscopy (ICP-OES), Fourier Transform Infrared Spectroscopy (FTIR) and Scanning Electron Microscopy (SEM) analysis. Antibacterial activity was tested against three commonly occurring bacteria known to colonize biomaterials, *i.e.* MRSA, *Staphylococcus aureus* and *Escherichia coli.*

Materials and methods

Materials

All materials, including GG (G1910, "Low-Acyl", 200-300 kD), calcium glycerophosphate (CaGP, 50043) and alkaline phosphatase (P7640), formic acid (purity >98%) gallic acid (purity >97.5%), catechin (purity >96%), caffeic acid (purity >95%), chlorogenic acid (purity >95%), luteolin (purity >98%), naringenin (98% purity), isorhamnetin (99% purity) were acquired from Sigma-Aldrich, unless stated otherwise. HPLC-grade methanol, water and acetonitrile were supplied by Fisher Scientific Chemicals (Loures, Portugal) and further filtered using a Solvent Filtration Apparatus 58061 from Supelco (Bellefonte, PA, USA). EGCG-rich extract (Green tea polyphenol extract, extracted by liquid/solid extraction, using water as solvent for the extraction, followed by purification with ethanol. EGCG > 65% (according to specification and information from manufacturer) was obtained from Oskar Tropitzsch e. K. Germany, PI extract (Pycnogenol®, from *Pinus pinaster*) was acquired from Biolandes Arômes, France and RO extract (Aquarox®, from *Rosmarinus officinalis*) from Vitiva, Slovenia.

Extract analysis

Extracts were analyzed by UHPL-DAD-MS^n. Extracts were dissolved in methanol HPLC grade (2–10 mg/mL) and filtered through a 0.2 µm PTFE syringe filter before injection (5 µL). The UHPLC system comprised a variable loop Accela autosampler (15°C), Accela 600 LC pump and Accela 80 Hz PDA detector (Thermo Fisher Scientific, San Jose, CA, USA). Compound separation was performed using a Hypersil Gold C_{18} (100 mm × 2.1 mm × 1.9 µm) column (Thermo Scientific, U.S.A.), at a flow rate of 0.42 mL/min and at 45°C. Mobile phase consisted of water/acetonitrile (99:1, v/v) (A) and acetonitrile (B), both with 0.1% formic acid. The following linear gradient was applied: 0-3 min: 1% B; 3-6 min: 1-5% B; 6-12 min: 5-10% B; 12-15 min: 10-15% B; 15-17 min: 15% B; 17-22 min: 15-20% B; 22-27 min: 20-25% B; 27-29 min: 25-50% B; 29-31 min: 50-100% B; 31-32 min: 100% B; 32-36 min: 100-1% B; followed by 4 min re-equilibration. Chromatograms at 280, 320 and 340 nm, and UV spectra from 200 to 600 nm were recorded.

UHPLC was coupled to a LCQ Fleet ion trap mass spectrometer (ThermoFinnigan, San Jose, CA, USA), as described before [15]. Capillary temperature was 275ºC and capillary and tune lens voltages were -41 V and -75 V, respectively.

Hydrogel preparation

GG hydrogel discs loaded with ALP and extract were prepared as described before [6] (FIG. 1a) and had final concentrations of 0.7% (w/v) GG, 0.03% (w/v) $CaCl_2$, 2.5 mg/mL ALP and 2.5 mg/mL of extract and were of 6 mm in diameter and 2.5 mm in height. GG, 0.1 M CaGP and ddH_2O were sterilized by autoclaving, $CaCl_2$, ALP and extract solutions by filtration (pore diameter 0.22 µm). ALP- and extract-loaded hydrogels were incubated in 0.1 M CaGP for 5 days (with refreshment after 1 and 3 days). Dry mass percentage was calculated as [(sample mass after drying)/(sample mass before drying)]x100%. SEM, ICP-OES and FTIR were performed as described before [6,16].

Antibacterial properties

For the minimal inhibitory concentration (MIC) test, MRSA was cultured in Mueller-Hinton broth (MH; Oxoid, Basingstoke, UK) at 37°C in aerobic conditions. The EUCAST broth microdilution protocol was used with flat-bottom 96-well plates (TPP, Trasadingen, Switzerland). The inoculum was standardized to approximately 5×10^5 Colony Forming Units (CFU)/mL. Extract concentrations ranging from 1024 µg/mL to 0.5 µg/mL were examined. After incubation at 37°C for 24 h, optical density was measured at 590 nm. MIC was defined as the lowest extract concentration at which the inoculated and the blank wells displayed similar optical densities.

After determining bactericidal activity by MIC measurement, antibacterial properties of the ALP- and extract loaded hydrogels post-mineralization were tested using the Kirby-Bauer diffusion test [17]. A hydrogel was placed in the middle of a 9 cm diameter Petri dish. 18 mL Mueller-Hinton agar (MHA) containing $1x10^7$ CFU/mL bacteria solidified in the dish over the hydrogel. After 24 h incubation under aerobic conditions at 37°C, the diameter of the inhibition growth zone was measured. *E. coli* (L70A4), *MRSA* (07001) and *S. aureus* (CIP224) were used.

Results and Discussion

Characteristics of extracts by UHPLC-DAD-MS^n

The phenolic fraction of EGCG-rich, PI and RO extracts were detailed characterized by UHPLC-DAD-MS^n analysis (TABLE 1). Phenolic compounds were identified based on their retention time, UV spectra and MS^n fragmentation pathway, comparing them with reference compounds or, when these were not available, with the literature. Quantification was performed using calibration curves of standards representative of each phenolic compound family (TABLE 2).

One phenolic acid and six flavanols were identified in EGCG-rich extract, namely gallic acid, two (epi)gallocatechin (EGC) isomers, catechin, two (epi)gallocatechin gallate (EGCG) isomers and (epi)catechin gallate (ECG) (TABLE 1). (Epi)gallocatechin gallate (EGCG) isomers were the major components found, accounting for 387.20 ± 15.53 mg/g and 181.96 ± 6.73 mg/g of the extract, respectively (TABLE 3). These results are consistent with the findings of Del Rio et al [23]. PI extract was shown to consist of quinic acid, protocatechuic acid, two B-type proanthocyanidin dimer isomers, catechin, caffeic acid, taxifolin-*O*-hexoside and taxifolin (TABLE 1). These compounds are well known constituents of pine bark extracts [24,25]. Quinic acid (26.95 ± 0.92 mg/g of the extract) and one B-type proanthocyanidin dimer (6.05 ± 0.44 mg/g of the extract) were shown to be the major components (TABLE 3).

In the same way, eighteen components were identified in RO extract (TABLE 1), namely quinic, syringic and caffeic and chlorogenic acids and three luteolin-*O*-rutinoside isomers, rosmarinic acid-glucoside, isorhamnetin-3-*O*-hexoside, apigenin-7-*O*-glucoside, rosmarinic acid, hesperetin-7-*O*-rutinoside, luteolin-7-*O*-glucuronide, three luteolin-3-*O*-(2''-*O*-acetyl)-b-D-glucuronide isomers, isorhamnetin-*O*-rutinoside and apigenin. Hesperetin-7-*O*-rutinoside and apigenin-7-*O*-glucoside were shown to be the major components of RO extract, accounting for 43.14 ± 1.09 mg/g and 20.16 ± 1.00 mg/g of the extract, respectively (TABLE 3). This in contrast to the findings of other authors who reported rosmarinic acid, carnosol and carnosic acid as the major compounds of rosemary extract [14,26]. Considering the total content of phenolic compounds, EGCG-rich extract showed the highest content (635.31 ± 19.31 mg/g of extract), followed by RO extract (112.59 ± 2.60 mg/g of extract) and by PI extract (49.99 ± 0.82 mg/g of extract).

TABLE 1. Phenolic compounds identified in EGCG-rich, PI and RO extracts and their corresponding retention time and MS^n fragmentation profile data.

EGCG-rich extract				
Rt (min)	**Compound**	**$[M-H]^-$ (*m/z*)**	**MS^n product ions (*m/z*)**	**Ref.**
1.34	Gallic acid	169	MS^2: 169(100)	Co[a]
2.41	(epi)gallocatechin isomer	305	MS^2: 287(15), 261(40), 221(90), 219(100), 179(100), 165(35), 137(30), 125(35)	[18]
6.09	(epi)gallocatechin isomer	305	MS^2: 287(15), 261(40), 221(90), 219(95), 179(100), 165(30), 137(25), 125(30)	[18]
6.78	Catechin	289	MS^2: 245(100), 205(35), 203(20), 179(20)	Co
9.75	Epigallocatechingallate isomer	457	MS^2: 331(95), 305(45), 287(15), 269(10), 193(25), 169(100)	[18]
11.40	Epigallocatechingallate isomer	457	MS^2: 331(100), 305(50), 287(15), 269(10), 193(20), 169(90)	[18]
14.50	(epi)catechin gallate	441	MS^2: 331(20), 289(100)271(15), 193(10), 169(20)	[18]
PI extract				
Rt (min)	**Compound**	**$[M-H]^-$ (*m/z*)**	**MS^n product ions (*m/z*)**	**Ref.**
0.68	Quinic acid	191	MS^2: 173(30), 127(10), 111(100), 93(10), 85(40)	[19]
2.55	Protocatechuic acid	153	MS^2: 109(100)	Co
6.28	Protanthocyanidin B-type dimer	577	MS^2: 451(60), 425(100), 407(60), 289(50); MS^3[289]: 245 (100)	[20]
6.71	Protanthocyanidin B-type dimer	577	MS^2: 559(20), 441(20), 425(100), 407(60), 289(20); MS^3[289]: 245 (100)	[20]
6.79	Catechin	289	MS^2: 289(100), 205(40), 203(20), 179(20)	Co
7.32	Caffeic acid	179	MS^2: 135(100)	Co
12.99	Taxifolin-*O*-hexoside	465	MS^2:447(40), 437(70), 303(30), 285(100), 259(40); MS3[303]: 285(100), 177(15), 151(10), 125(10); MS3[285]: 257(25), 241(100), 217(55), 199(20), 175(40), 163(15)	
13.28	Taxifolin	303	MS^2: 285(100), 177(10); MS3[285]: 257(15), 241(100), 217(15), 199(25), 175(60)	[19]
RO extract				
Rt (min)	**Compound**	**$[M-H]^-$ (*m/z*)**	**MS^n product ions (*m/z*)**	**Ref.**
0.68	Quinic acid	191	173 (60), 129 (20), 127 (60), 111 (40), 93 (50), 85 (100)	[19]
2.44	Syringic acid	197	MS^2:179 (100), 135 (10)	[21]
7.47	Caffeic acid	179	161(10), 135(100)	Co
8.70	Chlorogenic acid	353	MS^2:191(20), 179(60), 173(100), 135(30)	Co
16.20	Luteolin-*O*-rutinoside isomer	593	MS^2: 285(100); MS^3[285]: 267(20), 241(80), 199(95), 175(100), 151(25)	[22]
16.88	Rosmarinic acid glucoside	521	MS^2: 359(100), 323(20)	[21]
17.04	Isorhamnetin-3-*O*-hexoside	477	MS^2: 462(10), 357(10), 315(100), 300(20); MS^3[315]:300(100)	[22]
18.18	Apigenin-7-*O*-glucoside	431	MS^2: 269(100), 268(20)	[22]
18.71	Rosmarinic acid	359	MS^2:223(10), 197(30), 179(30), 161(100)	[22]
19.42	Hesperetin-7-*O*-rutinoside	609	MS^2: 301(100), 285(20); MS^3[301]: 286(100), 283(60), 257(40), 242(80), 227(30), 215(20), 199(50), 125(20)	[22]
19.57	Luteolin-7-*O*-glucuronide	461	MS^2: 446(20), 299(30), 285(100); MS^3[285]: 267(40), 257(20), 241(100), 217(85), 199(90), 175(90), 151(40)	[22]
21.95	Luteolin-3-*O*-(2"-*O*-acetyl)-b-D-glucuronide isomer 1	503	MS^2: 285 (100); MS^3 [285]: 257(25), 241(100), 217(70), 199(100), 175(90), 151(60), 137 (15)	[19,21]
22.27	Luteolin-3-*O*-(2"-*O*-acetyl)-b-D-glucuronide isomer 2	503	MS^2: 443(10), 285 (100); MS^3 [285]: 257(30), 241(100), 217(80), 199(90), 175(80), 151(30)	[19,21]
22.79	Luteolin-*O*-rutinoside isomer	593	MS^2: 285(100); MS^3[285]: 267(100), 241(30), 240(40), 199(10), 185(50), 175(20)	[22]
24.44	Luteolin-3-*O*-(2"-*O*-acetyl)-b-D-glucuronide isomer 3	503	MS^2: 285 (100); MS^3 [285]: 257(30), 241(60), 217(100), 199(60), 175(80), 151(20)	[19,21]
24.38	Isorhamnetin-*O*-rutinoside	623	MS^2: 315(100), 300(70); MS^3 [315]: 300(100)	[22]
24.55	Luteolin-*O*-rutinoside isomer	593	MS^2: 285(100); MS^3[285]: 267(70), 257(80), 241(90), 199(100), 175(60), 151(50)	[22]
25.77	Apigenin	269	MS^2: 241(10), 227(20), 225(100), 201(30), 197(15), 181(20), 151(30)	[19]

[a] Identified by co-injection of standard

TABLE 2. Calibration data used for the quantification of phenolic compounds in EGCG-rich, PI and RO extracts.

Compound	λ (nm)	Conc. Range (µg/mL)	Calibration curve[a]	*R2*	LOD[b]	LOQ[b]
Gallic acid	280	5.2-62.4	*y* = -270843+159824*x*	0.9918	6.4	21.2
Catechin	280	5.1-61.2	*y* = -189194+46707*x*	0.9943	5.8	19.4
Caffeic acid	320	5.3-63.6	*y* = -372767+460017*x*	0.9927	6.1	20.4
Chlorogenic acid	280	5.8-19.4	*y* = -340173+96071*x*	0.9928	5.8	19.4
Luteolin	340	2.6-31.2	*y* = -393592+298270*x*	0.9943	2.7	8.9
Naringenin	280	5.1-51.0	*y* = -193351+390536*x*	0.9573	16.0	53.2
Isorhamnetin	340	4.4-44.0	*y* = -9218+220419*x*	0.9531	12.1	40.3

[a] *y* = peak area, *x* = concentration in µg/mL
[b] LOD – limit of detection, LOQ – limit of quantification, both expressed as µg/mL

TABLE 3. Phenolic compounds content in EGCG-rich, PI and RO extracts, expressed in mg/g of extract.

Rt	Compound	EGCG-rich	PI	RO
0.68	Quinic acid[a]	-	26.95 ± 0.92	7.46 ± 0.46
1.34	Gallic acid[a]	4.72 ± 0.33	-	-
2.44	Syringic acid[a]	-	-	2.19 ± 0.15
2.49	(Epi)gallocatechin isomer[b]	<LOQ	-	-
2.55	Protocatechuic acid[a]	-	1.81 ± 0.08	-
6.28	Proanthocyanidin B-typer dimer[b]	-	4.40 ± 0.40	-
6.46	(Epi)gallocatechin isomer[b]	16.75 ± 0.58	-	-
6.71	Proanthocyanidin B-typer dimer[b]	-	6.05 ± 0.44	-
7.06	Catechin[b]	8.46 ± 0.48	5.04 ± 0.35	-
7.47	Caffeic acid[c]	-	1.57 ± 0.09	1.55 ± 0.09
8.70	Chlorogenic acid[d]	-	-	<LOQ
9.84	(Epi)gallocatechin gallate isomer[b]	181.96 ± 6.73	-	-
11.19	(Epi)gallocatechin gallate isomer[b]	387.20 ± 15.53	-	-
12.99	Taxifolin-*O*-hexoside[e]	-	2.97 ± 0.06	-
13.28	Taxifolin[e]	-	1.20 ± 002	-
14.72	(Epi)catechin gallate[b]	36.22 ± 2.08	-	
16.20	Luteolin-*O*-rutinoside isomer[f]	-	-	1.64 ± 0.08
16.88	Rosmarinic acid glucoside[c]	-	-	2.82 ± 0.14
17.04	Isorhamnetin-3-*O*-hexoside[e]	-	-	2.32 ± 0.08
18.18	Apigenin-7-*O*-glucoside[f]	-	-	20.16 ±1.00
18.71	Rosmarinic acid[c]	-	-	3.50 ± 0.25
19.42	Hesperetin-7-*O*-rutinoside[g]	-	-	43.14 ± 1.09
19.57	Luteolin-7-*O*-glucuronide[f]	-	-	6.32 ± 0.15
21.95	Luteolin-3-*O*-(2”-*O*-acetyl)-b-D-glucuronide isomer[f]	-	-	4.59 ± 0.25
22.27	Luteolin-3-*O*-(2”-*O*-acetyl)-b-D-glucuronide isomer[f]	-	-	5.57 ± 0.18
22.79	Luteolin-*O*-rutinoside isomer[f]	-	-	2.66 ± 0.20
24.44	Luteolin-3-*O*-(2”-*O*-acetyl)-b-D-glucuronide isomer[f]	-	-	3.72 ± 0.25
24.55	Isorhamnetin-*O*-rutinoside[e]	-	-	1.31 ± 0.09
24.93	Luteolin-*O*-rutinoside isomer[f]	-	-	1.83 ± 0.06
25.77	Apigenin[f]	-	-	1.82 ± 0.10
	TOTAL	**635.31 ± 19.31**	**49.99 ± 0.82**	**112.59 ± 2.60**

Results correspond to the average±standard deviation estimated from the injection of three aliquots analyzed in triplicate
Calibrations curves used:
[a]Gallic acid, 280 nm
[b]Catechin acid, 280 nm
[c]Caffeic acid, 320 nm
[d]Chlorogenic acid, 280 nm
[e]Isorhamnetin, 340 nm
[f]Luteolin, 340 nm
[g]Naringenin, 280 nm

Hydrogels mineralization: dry mass percentage and ICP-OES analysis

GG hydrogels were prepared with the same mass of extract per unit mass of hydrogel to ensure addition of equal masses of extract (FIG. 1a). Hydrogel mineralization led, as expected, to increased opacity (FIG. 1b), due to the formation of CaP inside the hydrogel. Extract-free hydrogels were white. Hydrogels loaded with EGCG-rich extract were light pink. PI-loaded hydrogels were distinctly pink and RO-loaded hydrogels were yellow.

Dry mass percentage values (FIG. 1c) were markedly higher for hydrogels loaded with EGCG-rich extract. ICP-OES results (FIG. 1d) confirmed higher amounts of Ca and P in hydrogels loaded with EGCG-rich extract, indicating the highest level of mineralization for this group as the Ca:P ratio was markedly higher in this group.

The observed color development of the hydrogels suggests interactions between extract components and ALP, as was recently described for algae extracts in hydrogels [13]. Light and dark pink color development in GTE and in PI-loaded hydrogels (FIG. 1b) may be due to non-covalent interactions between ALP and EGCG in GTE, or between ALP and proanthocyanidins in PI, respectively. Interactions of proteins with polyphenols is a well described phenomenon and has also been observed, for example, for whey protein beta-lactoglobulin and EGCG [27,28]. In addition, anthocyanins are colorful pigments that alter between blue and red in dependence of the pH value [29], thus it is not necessarily an indicator for protein binding but rather the natural color of the pigments. The reasons for the development of the yellow color in RO-loaded hydrogels (FIG. 1b) remain unclear, although Bongartz et al. described that, depending on the pH value, the oxidation state and the type of interacting amino acid the color of a chlorogenic acid solution alters between green, red and yellow [30]. Similar mechanisms are possible for other phenolic acids such as rosmarinic acid. However, a detailed discussion is beyond the scope of this paper.

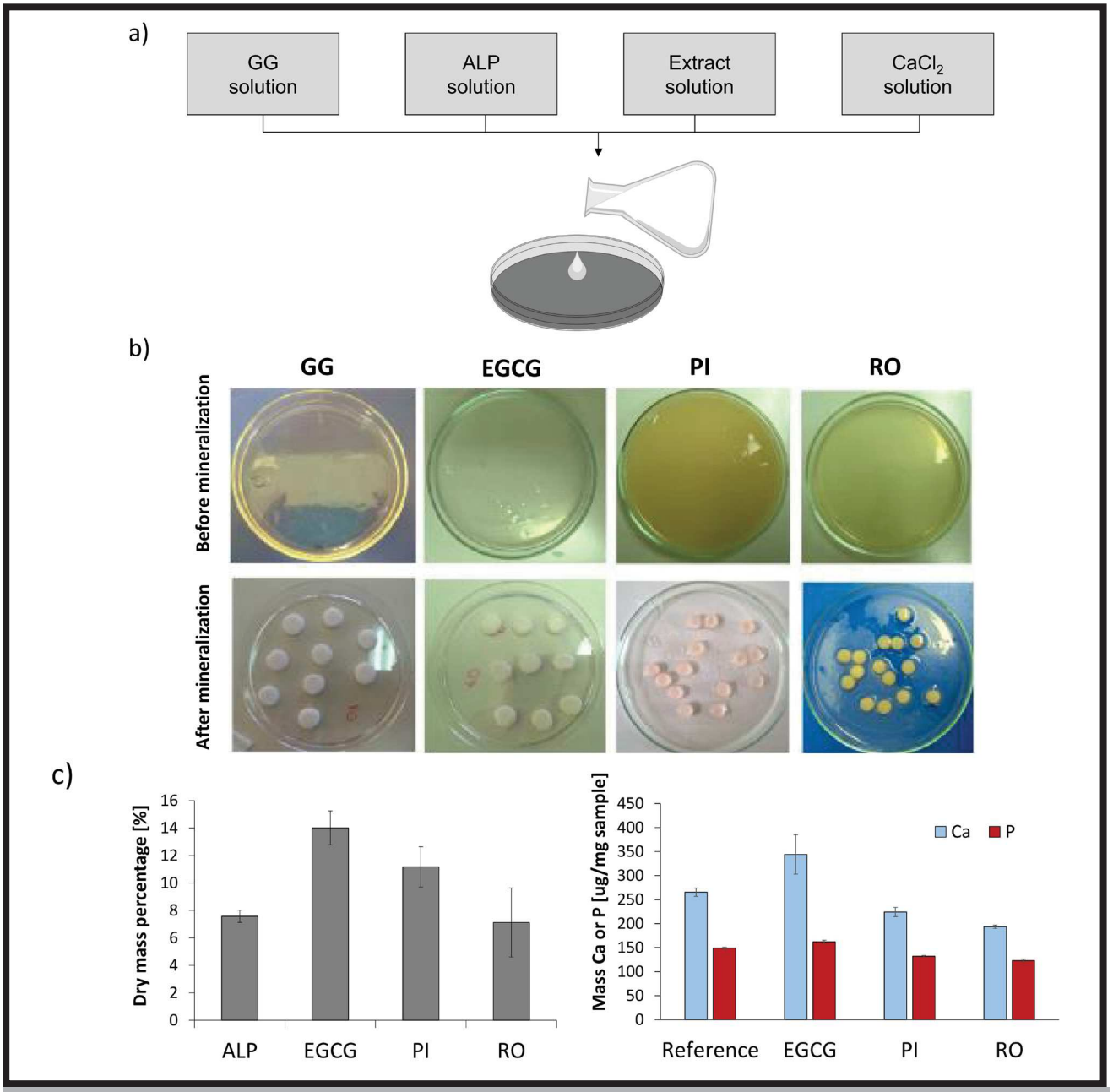

FIG. 1. (a) Method of production of extract-loaded GG hydrogels containing ALP; (b) Reference sample (GG) and samples with added extracts, *i.e.* EGCG-rich extract, PI and RO, before and after mineralization; (c) Dry mass percentage; (d) ICP-OES determination of mass of elemental Ca and P per unit mass hydrogel (µg/mg).

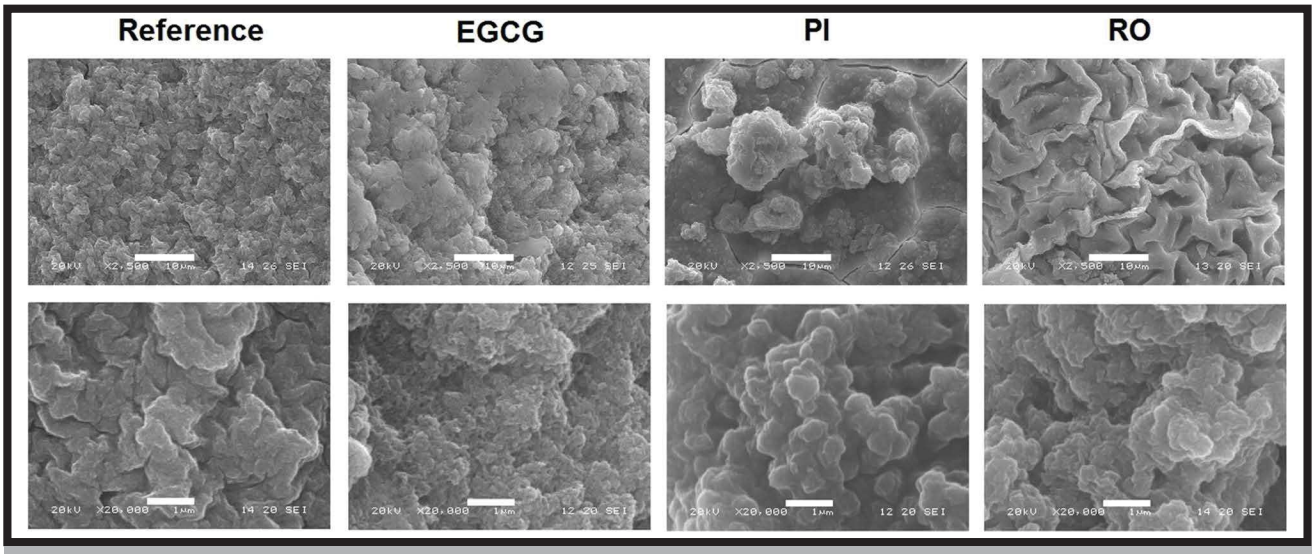

FIG. 2. SEM images of reference sample (GG) and samples with added extracts, i.e. EGCG-rich, PI and RO after mineralization. Top: magnification x2500. Bottom: magnification x20000. Scale bar: 10 μm (top), 1 μm (bottom).

The reasons why the EGCG-rich extract, promotes mineralization (FIG. 1c, 1d) may be hypothesized due to the binding of Ca^{2+} to EGCG, as EGCG has shown to form complexes with Ca^{2+} and proteins, which could stimulate CaP crystal nucleation [31]. Another possible explanation might be formation of complexes between polyphenols in the EGCG-rich extract and ALP, which could cause aggregation of ALP molecules or cause deformation leading to an increase in hydrodynamic diameter. Aggregation and increased hydrodynamic diameter would hinder ALP's diffusion from the hydrogel. This would increase intra-hydrogel ALP concentration, promoting CaP formation. The EGCG-rich extract contained a higher amount of phenolic compounds than the RO and PI extracts (TABLE 3). This may explain why the EGCG-rich extract promoted mineralization to a greater extent.

SEM and FTIR analysis

SEM microphotographs (FIG. 2) revealed a morphology consisting of mineral agglomerates on the surfaces of all mineralized hydrogels; thus, confirming their mineralization. The deposits were of sizes similar to those observed in GG hydrogels mineralized with ALP in previous works [32,33].

FTIR spectra (FIG. 3) confirmed mineralization by revealing bands characteristic for phosphate at 1100-1000 cm^{-1} (ν_3 stretching). Extract-loaded hydrogels exhibited a band at 870 cm^{-1}, corresponding to the ν_5 P–O(H) deformation of hydrogen phosphate groups, indicating formation of calcium-deficient hydroxyapatite (CDHA). In the case of EGCG-rich extract, the characteristic ν_3 stretching and ν_5 P–O(H) deformation bands were more pronounced. This finding and the higher Ca:P ratio in this group, suggest that the CDHA formed in the presence of this extract was of a higher degree of crystallinity. This outcome is consistent with previous work on enzymatic mineralization of catechol-PEG hydrogels [34], which revealed that presence of catechol groups displaying an affinity for Ca^{2+} ions and hydroxyapatite resulted in the highest degree of crystallinity [35,36].

The broad absorption band at approximately 3250 cm^{-1} indicated the presence of the O-H hydroxyl group, while the smaller bands at approximately 2900 and 2850 cm^{-1}, are due to C-H bending and the carboxyl -COOH group, respectively, while the bands at approximately 1675 cm^{-1} and 1040 cm^{-1} are due to the C-O carbonyl group from the glycosidic bond and the presence of a C-O-C ester group, respectively [37].

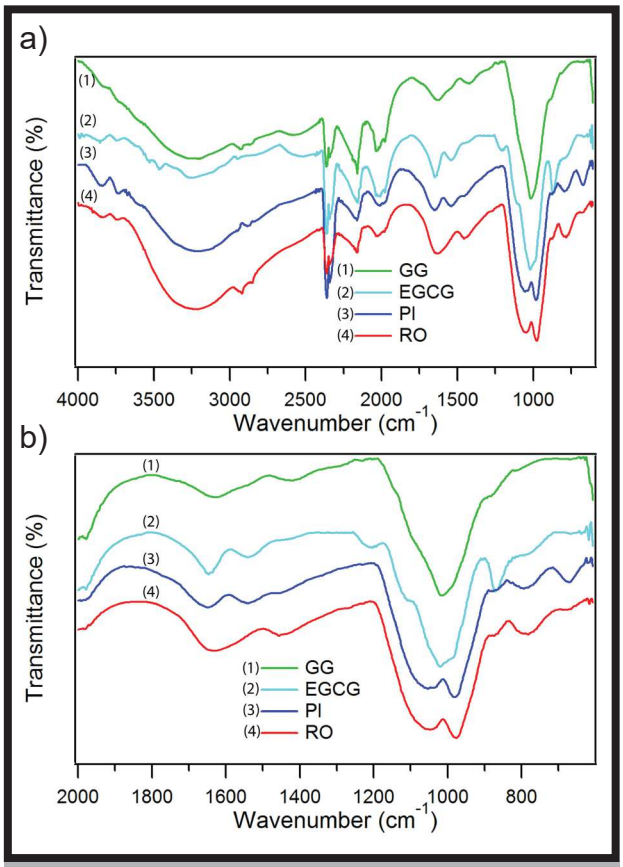

FIG. 3. FTIR spectra in the range 400-4000 cm^{-1} (a) and 400-2000 cm^{-1} (b) of reference GG hydrogels and GG hydrogels loaded with EGCG-rich, PI and RO extracts post-mineralization.

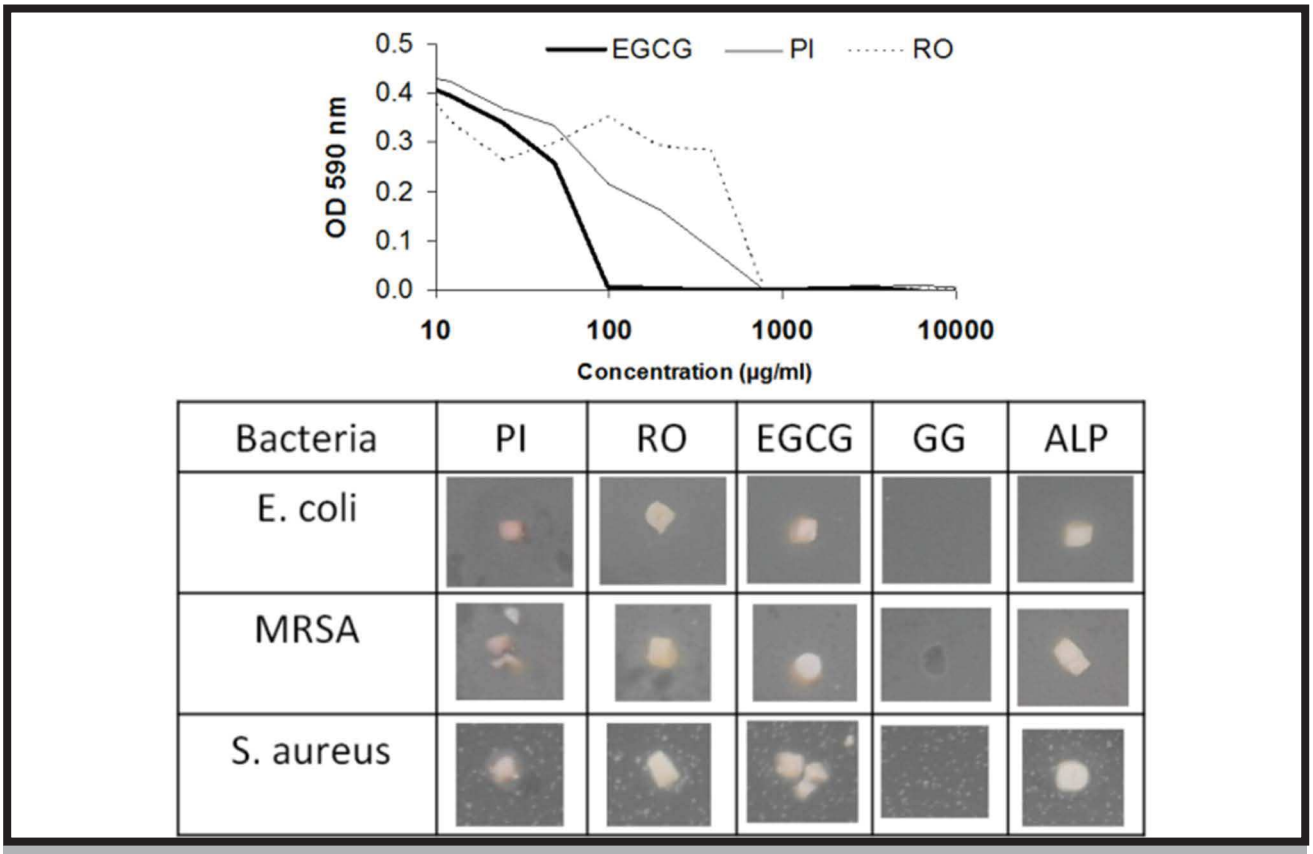

FIG. 4. Top: Minimal inhibitory concentration (MIC) of EGCG-rich, PI and RO extracts. Bottom: Representative images of the effect of the direct contact of the different hydrogels loaded with extracts post mineralization on growth of bacteria. GG: reference gellan gum hydrogel containing no extract or ALP. ALP: gellan gum hydrogel containing no extract.

Antibacterial properties

The minimal inhibitory concentration (MIC) test (FIG. 4) showed that all extracts, *per se*, lowered bacterial number, demonstrating antibacterial activity in the following order EGCG-rich > PI > RO.

The antibacterial activity in the order EGCG-rich > PI > RO (FIG. 4a) would be related with the higher quantity of phenolic compounds observed in EGCG-rich extracts, together with stronger antibacterial action of their components, namely EGC, catechin, EGCG and ECG (TABLE 1), which have been reported to be antibacterial towards *S. aureus* [38-40]. The PI extract displayed lower antibacterial activity. The polyphenols it contained (TABLE 1) have been reported to show different efficacies against *S. aureus*. Quinic acid, the major component found in PI extract, is reportedly ineffective against MRSA [41]. However, catechin, the B-type proanthocyanidin dimers or even other unidentified substances should be responsible for the antibacterial activity of this extract. RO extract displayed the lowest antibacterial activity against MRSA, although some of their components, such as apigenin derivatives and rosmarinic acid, have been reported to have considerable activity against *S. aureus* and MRSA [42].

Although solutions of the extracts themselves displayed antibacterial activity, antibacterial testing of extract-loaded hydrogels post-mineralization (FIG. 4) revealed that no zone of growth inhibition could be observed around any mineralized hydrogel discs, demonstrate lack of activity against any bacterial strain.

The lack of antibacterial activity of mineralized hydrogels (FIG. 4b) may be because bactericidal polyphenols and phenolic acids diffused out of the hydrogel during mineralization and/or become entrapped in the mineralized hydrogel. Hence the concentration of remaining polyphenols is below the MIC and hence too low to kill bacteria. Conceivably, a larger initial extract concentration should be used to guarantee antimicrobial activity after mineralization.

Further work will focus on cell biological characterization with bone-forming cells. It is believed that polyphenol-rich plant extracts will probably display minimal toxicity as they are used in traditional medicines but it is also believed that interactions of polyphenols with enzymes in eukaryotic cells is selective [9]. Therefore, in-depth testing is required.

Conclusion

In conclusion, EGCG-rich extract promoted hydrogel mineralization. EGCG-rich, PI and RO extracts all exhibited antibacterial activity against MRSA. Nevertheless, extract-loaded hydrogels post-mineralization did not appreciably hinder growth of MRSA, *E. coli* and *S. aureus*.

Acknowledgement

This work was supported by FWO, Belgium [postdoctoral fellowship: T.E.L.D.], BOF UGent, ERA-Net Rus project "Intelbiocomp" [A.G.S.], National Science Center, Poland (UMO-2018/29/N/ST8/01544), AgroForWealth: Biorefining of agricultural and forest by-products and wastes: integrated strategic for valorization of resources towards society wealth and sustainability (CENTRO-01-0145-FEDER-000001), funded by Centro2020, through FEDER and PT2020 and FCT (Fundação para a Ciência e Tecnologia) (financial support of CICECO-Aveiro Institute of Materials, and POCI-01-0145-FEDER-007679 (FCT UID/CTM/50011/2019)), and the N8 Agrifood Pump Priming Grant "Food2Bone", Lancaster University.

References

[1] E.M. Ahmed, Hydrogel: Preparation, characterization, and applications: A review. J Adv Res 6(2) (2015) 105-21.
[2] S. Donatan, A. Yashchenok, N. Khan, B. Parakhonskiy, M. Cocquyt, B.E. Pinchasik, D. Khalenkow, et al.: Loading Capacity versus Enzyme Activity in Anisotropic and Spherical Calcium Carbonate Microparticles. Acs Applied Materials & Interfaces 8(22) (2016) 14284-14292.
[3] M. Maitra, V.K. Shukla: Cross-linking in Hydrogels - A Review. Am J Polym Sci 4(2) (2014) 25.
[4] D.F. Coutinho, S.V. Sant, H. Shin, J.T. Oliveira, M.E. Gomes, N.M. Neves, A. Khademhosseini, R.L. Reis: Modified Gellan Gum hydrogels with tunable physical and mechanical properties, Biomaterials 31(29) (2010) 7494-502.
[5] C.J. Ferris, K.J. Gilmore, G.G. Wallace, M.i.h. Panhuis: Modified gellan gum hydrogels for tissue engineering applications, Soft Matter 9(14) (2013) 3705-3711.
[6] T.E. Douglas, A. Dokupil, K. Reczynska, G. Brackman, M. Krok-Borkowicz, J.K. Keppler, M. Bozic, P. Van Der Voort, K. Pietryga, S.K. Samal, L. Balcaen, J. van den Bulcke, J. Van Acker, et al.: Enrichment of enzymatically mineralized gellan gum hydrogels with phlorotannin-rich Ecklonia cava extract Seanol((R)) to endow antibacterial properties and promote mineralization, Biomed Mater 11(4) (2016) 045015.
[7] J.R. Mediavilla, L. Chen, B. Mathema, B.N. Kreiswirth: Global epidemiology of community-associated methicillin resistant Staphylococcus aureus (CA-MRSA), Curr Opin Microbiol 15(5) (2012) 588-95.
[8] A.C. Uhlemann, M. Otto, F.D. Lowy, F.R. DeLeo: Evolution of community- and healthcare-associated methicillin-resistant Staphylococcus aureus, Infect Genet Evol 21 (2014) 563-74.
[9] T.P.T. Cushnie, A.J. Lamb: Antimicrobial activity of flavonoids, International Journal of Antimicrobial Agents 26(5) (2005) 343-356.
[10] A.N. Panche, A.D. Diwan, S.R. Chandra: Flavonoids: an overview, J Nutr Sci 5 (2016) e47.
[11] S. Swioklo, K.A. Watson, E.M. Williamson, J.A. Farrimond, S.E. Putnam, K.A. Bicknell: Defining Key Structural Determinants for the Pro-osteogenic Activity of Flavonoids, J Nat Prod 78(11) (2015) 2598-2608.
[12] Y. Yoda, Z.Q. Hu, W.H. Zhao, T. Shimamura: Different susceptibilities of Staphylococcus and Gram-negative rods to epigallocatechin gallate, J Infect Chemother 10(1) (2004) 55-8.
[13] E. Hames-Kocabas, O. Yesil-Celiktas, M. Isleten, F. Vardar-Sukan: Antimicrobial activity of pine bark extract and asssessment of potential application in cooked red meat, GIDA 33(3) (2008) 123-127.
[14] S. Moreno, T. Scheyer, C.S. Romano, A.A. Vojnov: Antioxidant and antimicrobial activities of rosemary extracts linked to their polyphenol composition, Free Radical Research 40(2) (2006) 223-231.
[15] R. Touati, S.A.O. Santos, S.M. Rocha, K. Belhamel, A.J.D. Silvestre: Phenolic composition and biological prospecting of grains and stems of Retama sphaerocarpa, Industrial Crops and Products 95 (2017) 244-255.
[16] T.E. Douglas, A. Lapa, K. Reczynska, M. Krok-Borkowicz, K. Pietryga, S.K. Samal, H.A. Declercq, D. Schaubroeck, M. Boone, P. Van der Voort, K. De Schamphelaere, C.V. Stevens, V. Bliznuk, L. Balcaen, B.V. Parakhonskiy, F. Vanhaecke, V. Cnudde, E. Pamula, A.G. Skirtach: Novel injectable, self-gelling hydrogel-microparticle composites for bone regeneration consisting of gellan gum and calcium and magnesium carbonate microparticles, Biomed Mater 11(6) (2016) 065011.
[17] A.W. Bauer, W.M. Kirby, J.C. Sherris, M. Turck: Antibiotic susceptibility testing by a standardized single disk method, Tech Bull Regist Med Technol 36(3) (1966) 49-52.
[18] D. Del Rio, A.J. Stewart, W. Mullen, J. Burns, M.E. Lean, F. Brighenti, A. Crozier: HPLC-MSn analysis of phenolic compounds and purine alkaloids in green and black tea, Journal of agricultural and food chemistry 52(10) (2004) 2807-2815.
[19] R. Touati, S.A. Santos, S.M. Rocha, K. Belhamel, A.J. Silvestre: Phenolic composition and biological prospecting of grains and stems of Retama sphaerocarpa, Industrial crops and products 95 (2017) 244-255.
[20] M. de la Luz Cádiz-Gurrea, S. Fernández-Arroyo, A. Segura-Carretero: Pine bark and green tea concentrated extracts: antioxidant activity and comprehensive characterization of bioactive compounds by HPLC–ESI-QTOF-MS, International journal of molecular sciences 15(11) (2014) 20382-20402.
[21] M. Achour, R. Mateos, M. Ben Fredj, A. Mtiraoui, L. Bravo, S. Saguem: A comprehensive characterisation of rosemary tea obtained from Rosmarinus officinalis L. collected in a sub-humid area of Tunisia, Phytochemical analysis 29(1) (2018) 87-100.
[22] P. Mena, M. Cirlini, M. Tassotti, K.A. Herrlinger, C. Dall'Asta, D. Del Rio: Phytochemical Profiling of Flavonoids, Phenolic Acids, Terpenoids, and Volatile Fraction of a Rosemary (Rosmarinus officinalis L.) Extract, Molecules 21(11) (2016).
[23] D. Del Rio, A.J. Stewart, W. Mullen, J. Burns, M.E. Lean, F. Brighenti, A. Crozier: HPLC-MSn analysis of phenolic compounds and purine alkaloids in green and black tea, J Agric Food Chem 52(10) (2004) 2807-15.
[24] H.A. Weber, A.E. Hodges, J.R. Guthrie, B.M. O'Brien, D. Robaugh, A.P. Clark, R.K. Harris, J.W. Algaier, C.S. Smith: Comparison of proanthocyanidins in commercial antioxidants: grape seed and pine bark extracts, J Agric Food Chem 55(1) (2007) 148-56.
[25] S. Iravani, B. Zolfaghari: Pharmaceutical and nutraceutical effects of Pinus pinaster bark extract, Res Pharm Sci 6(1) (2011) 1-11.
[26] E.N. Frankel, S.W. Huang, R. Aeschbach, E. Prior: Antioxidant activity of a rosemary extract and its constituents, carnosic acid, carnosol, and rosmarinic acid, in bulk oil and oil-in-water emulsion, Journal of Agricultural and Food Chemistry 44(1) (1996) 131-135.
[27] J.K. Keppler, D. Martin, V.M. Garamus, K. Schwarz: Differences in binding behavior of (-)-epigallocatechin gallate to -lactoglobulin heterodimers (AB) compared to homodimers (A) and (B), Journal of Molecular Recognition 28(11) (2015) 656-666.
[28] S. Wiese, S. Gartner, H.M. Rawel, P. Winterhalter, S.E. Kulling: Protein interactions with cyanidin-3-glucoside and its influence on alpha-amylase activity, Journal of the Science of Food and Agriculture 89(1) (2009) 33-40.
[29] H.E. Khoo, A. Azlan, S.T. Tang, S.M. Lim: Anthocyanidins and anthocyanins: colored pigments as food, pharmaceutical ingredients, and the potential health benefits, Food & Nutrition Research 61 (2017) 1-21.
[30] V. Bongartz, L. Brandt, M.L. Gehrmann, B.F. Zimmermann, N. Schulze-Kaysers, A. Schieber: Evidence for the Formation of Benzacridine Derivatives in Alkaline-Treated Sunflower Meal and Model Solutions, Molecules 21(1) (2016).
[31] F. Fuchs, Z. Grabarek: The green tea polyphenol (-)-epigallocatechin-3-gallate inhibits magnesium binding to the C-domain of cardiac troponin C, Journal of Muscle Research and Cell Motility 34(2) (2013) 107-113.
[32] T.E. Douglas, G. Krawczyk, E. Pamula, H.A. Declercq, D. Schaubroeck, M.M. Bucko, L. Balcaen, P. Van Der Voort, V. Bliznuk, N.M. van den Vreken, M. Dash, et al.: Generation of composites for bone tissue-engineering applications consisting of gellan gum hydrogels mineralized with calcium and magnesium phosphate phases by enzymatic means, J Tissue Eng Regen Med 10(11) (2016) 938-954.
[33] T.E.L. Douglas, M. Pilarz, M. Lopez-Heredia, G. Brackman, D. Schaubroeck, L. Balcaen, V. Bliznuk, P. Dubruel, C. Knabe-Ducheyne, F. Vanhaecke, T. Coenye, E. Pamula: Composites of gellan gum hydrogel enzymatically mineralized with calcium-zinc phosphate for bone regeneration with antibacterial activity, J Tissue Eng Regen Med 11(5) (2017) 1610-1618.
[34] T.E. Douglas, P.B. Messersmith, S. Chasan, A.G. Mikos, E.L. de Mulder, G. Dickson, D. Schaubroeck, L. Balcaen, F. Vanhaecke, P. Dubruel, J.A. Jansen, S.C. Leeuwenburgh: Enzymatic mineralization of hydrogels for bone tissue engineering by incorporation of alkaline phosphatase, Macromol Biosci 12(8) (2012) 1077-89.
[35] W.M. Chirdon, W.J. O'Brien, R.E. Robertson: Adsorption of catechol and comparative solutes on hydroxyapatite, J Biomed Mater Res B Appl Biomater 66(2) (2003) 532-8.
[36] J. Ryu, S.H. Ku, H. Lee, C.B. Park: Mussel-Inspired Polydopamine Coating as a Universal Route to Hydroxyapatite Crystallization, Adv. Funct. Mater. 20 (2010) 2132–2139.
[37] A.M. Jaafar, V .Thatchinamoorthi, Preparation and Characterisation of Gellan Gum Hydrogel containing Curcumin and Limonene, IOP Conf. Series: Materials Science and Engineering 440 (2018) 012023
[38] T.O. Ajiboye, M. Aliyu, I. Isiaka, F.Z. Haliru, O.B. Ibitoye, J.N. Uwazie, H.F. Muritala, S.A. Bello, I.I. Yusuf, A.O. Mohammed: Contribution of reactive oxygen species to (+)-catechin-mediated bacterial lethality, Chemico-Biological Interactions 258 (2016) 276-287.
[39] J.C. Anderson, R.A. McCarthy, S. Paulin, P.W. Taylor: Anti-staphylococcal activity and beta-lactam resistance attenuating capacity of structural analogues of (-)-epicatechin gallate, Bioorg Med Chem Lett 21(23) (2011) 6996-7000.
[40] B.S. Fazly Bazzaz, S. Sarabandi, B. Khameneh, H. Hosseinzadeh: Effect of Catechins, Green tea Extract and Methylxanthines in Combination with Gentamicin Against Staphylococcus aureus and Pseudomonas aeruginosa: - Combination therapy against resistant bacteria, J Pharmacopuncture 19(4) (2016) 312-318.
[41] C.O. Rezende, L.A. Oliveira, B. Oliveira, C.G. Almeida, B.S. Ferreira, M. Le Hyaric, G.S.L. Carvalho, M.C.S. Lourenco, M. Batista, F.K. Marchini, et al: Synthesis and Antibacterial Activity of Alkylated Diamines and Amphiphilic Amides of Quinic Acid Derivatives, Chemical Biology & Drug Design 86(3) (2015) 344-350.
[42] S.P. Ekambaram, S.S. Perumal, A. Balakrishnan, N. Marappan, S.S. Gajendran, V. Viswanathan: Antibacterial synergy between rosmarinic acid and antibiotics against methicillin-resistant Staphylococcus aureus, Journal of Intercultural Ethnopharmacology 5(4) (2016) 358-363.